Development 138, 5403-5414 (2011) doi:10.1242/dev.069849

Dual embryonic origin of the mammalian otic vesicle forming the inner ear

Laina Freyer[1,*], Vimla Aggarwal[2] and Bernice E. Morrow[1,3,*]

SUMMARY

The inner ear and cochleovestibular ganglion (CVG) derive from a specialized region of head ectoderm termed the otic placode. During embryogenesis, the otic placode invaginates into the head to form the otic vesicle (OV), the primordium of the inner ear and CVG. Non-autonomous cell signaling from the hindbrain to the OV is required for inner ear morphogenesis and neurogenesis. In this study, we show that neuroepithelial cells (NECs), including neural crest cells (NCCs), can contribute directly to the OV from the neural tube. Using *Wnt1-Cre*, *Pax3*$^{Cre/+}$ and *Hoxb1*$^{Cre/+}$ mice to label and fate map cranial NEC lineages, we have demonstrated that cells from the neural tube incorporate into the otic epithelium after otic placode induction has occurred. *Pax3*$^{Cre/+}$ labeled a more extensive population of NEC derivatives in the OV than did *Wnt1-Cre*. NEC derivatives constitute a significant population of the OV and, moreover, are regionalized specifically to proneurosensory domains. Descendents of *Pax3*$^{Cre/+}$ and *Wnt1-Cre* labeled cells are localized within sensory epithelia of the saccule, utricle and cochlea throughout development and into adulthood, where they differentiate into hair cells and supporting cells. Some NEC derivatives give rise to neuroblasts in the OV and CVG, in addition to their known contribution to glial cells. This study defines a dual cellular origin of the inner ear from sensory placode ectoderm and NECs, and changes the current paradigm of inner ear neurosensory development.

KEY WORDS: Inner ear, Neural crest cells, Fate mapping, Sensory placode, Mouse

INTRODUCTION

Cranial sensory placodes are thickenings of ectoderm that are the source of complex sensory organs and ganglia that innervate the head and neck (D'Amico-Martel and Noden, 1983; Le Douarin, 1986). The otic placode is induced next to the hindbrain and invaginates into the head to form the otic cup. The otic cup then closes off from the surface ectoderm of the head, thus creating the OV (Anniko and Wikstrom, 1984). Neuroblasts are specified within the otic epithelium and delaminate into the mesenchyme where they condense to form the CVG (Wikstrom and Anniko, 1987; Ma et al., 1998). The OV undergoes morphogenesis to give rise to the inner ear labyrinth, a continuous epithelium that makes up the vestibular [endolymphatic duct (ED), semicircular canals (SCC), utricle, saccule] and auditory (cochlea) components of the inner ear (Morsli et al., 1998). This is accompanied by development of six sensory patches: three cristae (at the base of each SCC), two maculae (utricular, saccular) and the organ of Corti (within the cochlea). Sensory epithelia are defined by the presence of mechanosensory hair cells that are associated with supporting cells and innervated by CVG neurons.

To date, it is widely accepted that the otic placode ectoderm is the only source for the inner ear labyrinth and neurons of the CVG (for reviews, see Fekete and Wu, 2002; Barald and Kelley, 2004). Contributions of other tissues to inner ear development include melanocytes, which are derived from NCCs. NCCs are specified in the dorsal neural tube and migrate throughout the embryo (Bronner-Fraser, 1995; Graham et al., 2004). Cranial NCC migratory streams are organized by rhombomeric segments of the hindbrain and respond to cues from the pharyngeal endoderm (Graham et al., 2004; Birgbauer et al., 1995; Sauka-Spengler and Bronner-Fraser, 2008). In mice, melanocyte progenitor cells originate from the midbrain-hindbrain junction and cervical trunk regions of the neural tube, and then migrate around the inner ear later in development to give rise to the intermediate cells of the stria vascularis (SV) that is located along the lateral wall of the cochlea (Wilson et al., 2004; Steel and Barkway, 1989; Cable et al., 1992; Cable et al., 1995). We decided to examine other potential functions of NCCs in inner ear development.

In this study, we used *Wnt1-Cre*, *Pax3*$^{Cre/+}$ and *Hoxb1*$^{Cre/+}$ mice to genetically fate map GFP-expressing reporter cells from the neural tube. Although *Wnt1-Cre* has been widely used to fate map NCCs, we found that *Pax3*$^{Cre/+}$ labeled a broader population of NECs in the neural tube, including NCCs. Our fate-mapping results demonstrate that NEC/NCC derivatives contribute a significant population of cells to the inner ear. Using time-lapse microscopy, we documented *Pax3*$^{Cre/+}$ labeled cells invading the otic epithelium in vivo. NEC descendants remain in the inner ear throughout development and localize to the CVG and sensory epithelia of the utricle, saccule and cochlea where they are distinct from pigment-producing melanocytes. *Wnt1-Cre* and *Pax3*$^{Cre/+}$-labeled reporter cells in the CVG express the early neuroblast markers NeuroD and Islet-1. *Pax3*$^{Cre/+}$ derivatives differentiate into hair cells that express myosin VIIA (MyoVIIA) and supporting cells that express the Ca^{2+}-binding protein S100 or the neurotrophin receptor P75. In adult mice, *Pax3*$^{Cre/+}$-labeled derivatives persist in the CVG, maculae and cochlea. Our fate-mapping results confirm an NEC origin of glial cells in the CVG that express Sox10, along with some *Pax2-Cre*-labeled derivatives that also express Sox10 in the CVG.

[1]Department of Genetics, Albert Einstein College of Medicine, 1301 Morris Park Avenue, Bronx, NY 10461, USA. [2]Department of Pediatrics, Columbia University Medical Center, 622 West 168th Street, New York, NY 10032, USA. [3]Departments of Ob/Gyn and Pediatrics, Albert Einstein College of Medicine, 1301 Morris Park Avenue, Bronx, NY 10461, USA.

*Authors for correspondence (bernice.morrow@einstein.yu.edu; laina.freyer@phd.einstein.yu.edu)

Accepted 18 October 2011

MATERIALS AND METHODS

Mouse models

Mice were used in this study according to the regulatory standards of the Institutional Animal Care and Use Committee (IACUC) of Albert Einstein College of Medicine. All mouse lines used in this study have been previously described. *Pax3*$^{Cre/+}$ (stock number 005549), *Wnt1-lacZ* (stock number 002865) and *Hoxb1*$^{Cre/+}$ (stock number 012373) mice were purchased from Jackson Laboratories. *RCE:LoxP* mice were obtained from Dr Gordon Fishell (NYU Langone Medical Center, NY, USA). Sequences of primers used for PCR genotyping are in supplementary material Table S1. Embryos were dissected according to date of vaginal plug (considered to be E0.5). Embryonic stage was confirmed by counting somite pairs.

Direct fluorescence

GFP was detected by direct fluorescence. Whole-mount images were taken immediately following dissection. For tissue sections, embryos were fixed accordingly: 2 hours for ≤10.5, 4 hours for E11.5, and overnight for ≥E12.5. E17.5 embryos and adults required removal of the temporal bone for overnight fixation. Fixation was carried out in 4% paraformaldehyde (PFA) in PBS at 4°C. Adult inner ears required perfusion of the cochlea. After fixation, tissue was washed in phosphate-buffered saline (PBS) then cryoprotected in 30% sucrose in PBS overnight at 4°C. Adult inner ears were decalcified in 0.5 M EDTA in PBS (pH 8.0) at 4°C for 48 hours prior to sucrose. Tissue was embedded in OCT and cryosectioned at 12-14 μm.

X-gal staining

Whole embryos were fixed in 1% formaldehyde, 0.2% gluteraldehyde, 2 mM $MgCl_2$, 5 mM EGTA and 0.02% NP-40 in PBS. Fixation time varied with embryonic stage (15 minutes for E8.5, 20 minutes for E9.5, 30 minutes for E10.5). Embryos were stained in 5 mM $K_3Fe(CN)_6$, 5 mM $K_4Fe(CN)_6$, 2 mM $MgCl_2$, 0.01% deoxycholic acid, 0.02% NP-40 and 1 mg/ml X-gal in PBS at 4°C overnight. Embryos were post-fixed in 4% PFA and cryosectioned at 10 μm. Tissue sections were dehydrated in an ethanol series into xylene and mounted in Permount.

RNA in situ hybridization

For whole-mount RNA in situ hybridization, embryos were fixed in 4% PFA at 4°C overnight and dehydrated in a methanol series with PBS/0.1% Tween-20 and stored at –20°C. The detailed protocol for RNA in situ hybridization has been previously described (Franco et al., 2001). An RNA probe template for *Cre* was amplified by PCR from E10.5 *Wnt1-Cre* mouse cDNA using the following primers: CreT3Sense, 5′-GGGGAATTAACC-CTCACTAAAGGGGATGGACATGTTCAGGGATC-3′; CreT7AS, 5′-GGGGTAATACGACTCACTATAGGGCATTGCCCCTGTTTCACTATC-3′. PCR amplification adds T3 and T7 RNA polymerase-binding sites for digoxigenin-labeled sense and antisense probe generation, respectively. An antisense probe for *Crabp1* was synthesized with T7 polymerase from a pSE5 plasmid linearized with *Bam*HI (Dr Moises Mallo, Spain). For RNA in situ hybridization on sections, embryos were cryoembedded, sectioned at 14 μm, incubated at 30°C for 20 minutes then stored at –80°C. RNA in situ hybridization was performed on tissue sections according to a protocol developed in David Anderson's laboratory (California Institute of Technology, Pasadena, CA, USA).

Time-lapse intravital imaging

Dissections were performed such that the placenta was left intact and the amniotic sac was punctured so that the head of the embryo could be exposed. Embryos were counterstained with red-fluorescent wheat germ agglutinin (Invitrogen I34406) in 1× HBSS at 37°C for 10 minutes and embedded in 0.6% agarose in MatTek glass-bottom dishes. Time-lapse imaging was performed using an Olympus FV-1000-MPE multiphoton microscope and 25× water objective. Optical sectioning was at 5 μm and captured every 10 minutes for up to 3 hours. *Z*-series were reconstructed and movies compiled using ImageJ software.

Immunofluorescence on tissue sections

Embryos were fixed and sectioned as described for direct fluorescence. Sections were permeabilized in 0.5% Triton X-100 for 5 minutes. Blocking was performed with 5% serum (goat or donkey) in PBS/0.1% TritonX-100 (PBT) for 1 hour. Primary antibody was diluted in block and incubated for 1 hour. Primary antibodies were: anti-NeuroD (SCBT sc-1084, 1:500), anti-islet 1 (DSHB 39.4D5, 1:100), anti-neurofilament (DSHB 2H3, 1:100), anti-P75 (Promega G3231, 1:500), anti-S100 (DAKO Z0311, 1:500), anti-MyoVIIA (DSHB MYO7A 138-1, 1:500), anti-Sox10 (Santa Cruz sc-17342, 1:100), anti-Pax3 (DSHB, 1:50), anti-Pax2 (Invitrogen 71-6000, 1:50), anti-AP2α (DSHB 3B5, 1:100), anti-Snai1 (Antonio García de Herreros, IMIM Hospital del Mar Research Institute, Barcelona, Spain, 1:5) and anti-laminin (Millipore AB2034, 1:200). Sections were washed in PBT and incubated with secondary antibodies and DAPI (1:500) for 1 hour. Secondary antibodies were: Alexa Fluor 568 goat α-rabbit IgG (Invitrogen A11011, 1:500), Alexa Fluor 568 goat α-mouse IgG (Invitrogen A11004, 1:500) and Alexa Fluor 568 donkey α-goat IgG (Invitrogen A11057, 1:500). Slides were mounted in hard-set mounting medium (Vector Labs H-1400). Images of were captured using a Zeiss Axio Observer or Leica SP2 AOBS confocal microscope.

Immunofluorescence on whole-mount tissue

Sensory epithelia from the utricle, saccule and organ of Corti were exposed by microdissection of the surrounding tissue. Immunofluorescence was performed as described for tissue sections except that primary antibody (MyoVIIA) was incubated 1:10 overnight at 4°C. Tissue was embedded in 0.6% agarose/PBS in a MatTek glass-bottom dish for imaging with a Leica SP2 AOBS confocal microscope.

Paintfilling of the inner ear labyrinth

Embryos were cut below the forelimbs and fixed in 5% glacial acetic acid, 2% formaldehyde and 75% ethanol overnight. This was followed by dehydration to ethanol and clearing in methyl salicylate. Embryos were bisected dorsally and the brain was removed. A micropipette was used to microinject 0.2% correction fluid diluted in methyl salicylate into the utricle. Paintfilled inner ears were imaged and stored in methyl salicylate.

RESULTS

Fate mapping of NEC lineages to the mouse OV and CVG

Cranial NCCs emigrate from the neural tube during a developmental stage at which the otic cup is in direct contact with the hindbrain (Serbedzija et al., 1992; Schneider-Maunoury and Pujades, 2007). Close proximity of the OV to the neural tube allows for non-autonomous signaling from the hindbrain that is required for neurogenesis and morphogenesis (Liang et al., 2010). Direct cellular contribution of NECs from the hindbrain to the OV has not been investigated.

We genetically fate mapped NEC populations using *Wnt1-Cre* transgenic mice (Danielian et al., 1998), *Pax3*$^{Cre/+}$ knock-in mice (Engleka et al., 2005) and *Hoxb1*$^{Cre/+}$ knock-in mice (O'Gorman, 2005) together with a conditionally activated GFP reporter line (*RCE;loxP*, referred to as *RCE*$^{GFP/+}$) (Sousa et al., 2009) in order to further investigate the contribution of NECs to inner ear development. *Wnts* are secreted proteins that are necessary for NCC induction (Sauka-Spengler and Bronner-Fraser, 2008), and *Wnt1* expression is normally limited to the developing central nervous system (McMahon and Bradley, 1990). *Wnt1-Cre* is widely used to label NCC derivatives in mice and is active in neuroectoderm that forms the most dorsal part of the neural tube where NCC specification occurs (Fig. 1A). Pax3 is a paired box homeodomain transcription factor that is a downstream target of Wnt signaling in premigratory NCCs (Sauka-Spengler and Bronner-Fraser, 2008). *Pax3*$^{Cre/+}$ is also expressed in the neural tube (Fig. 1B), with additional expression in the somites (Engleka et al., 2005; Goulding et al., 1991). In early to mid-gestation, *Hoxb1*$^{Cre/+}$ expression is specific to rhombomere 4 in the anterior embryo (Fig. 1C). For comparison, we performed a fate map of the otic placode ectoderm lineage (Fig. 1D) as labeled by *Pax2-Cre* (Ohyama and Groves,

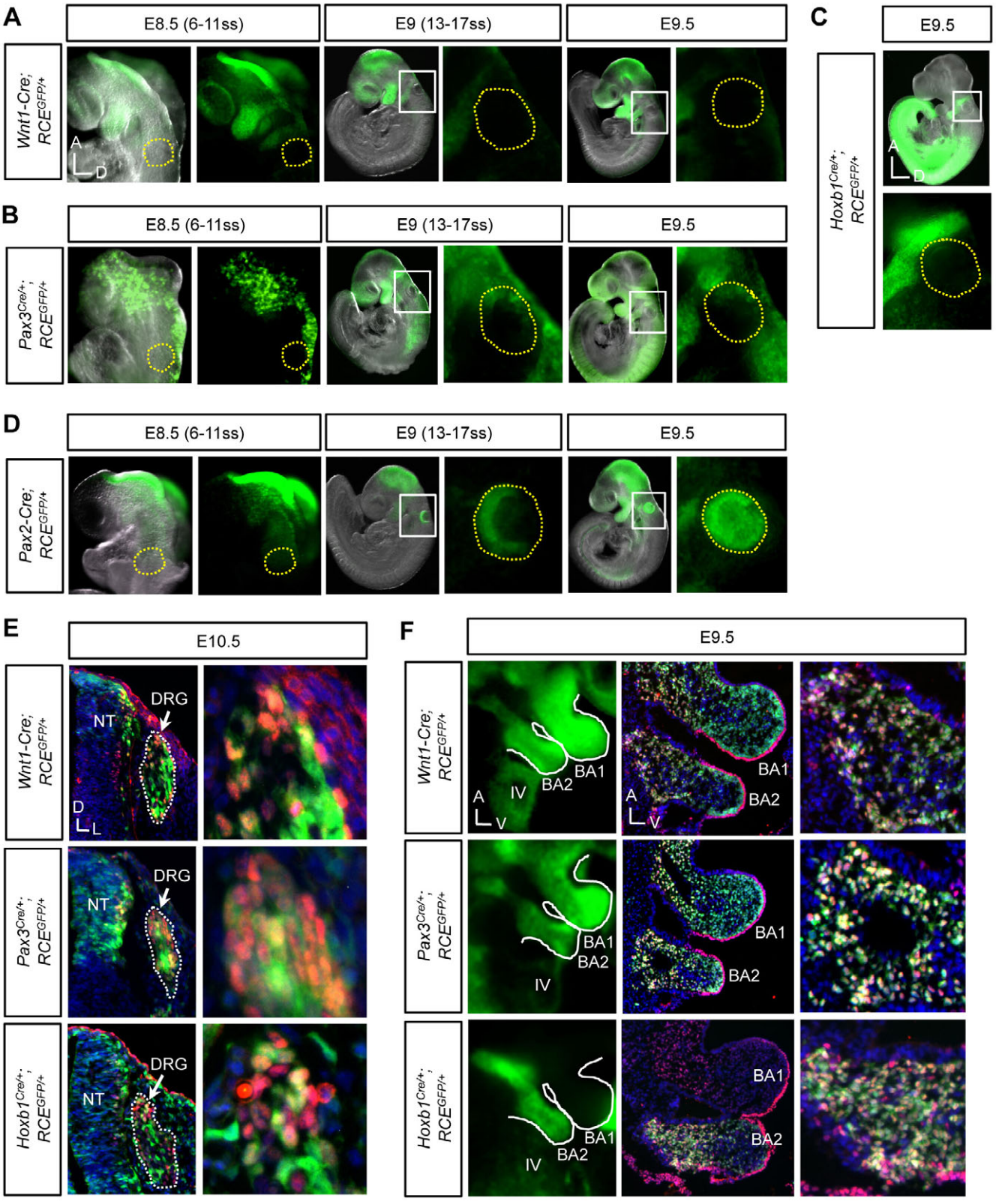

Fig. 1. Fate mapping of NEC/NCC and otic placode ectoderm populations. (**A-D**) Lateral views of whole-mount embryos from E8.5 to E9.5. GFP reporter expression is activated by *Wnt1-Cre*, *Pax3*$^{Cre/+}$, *Hoxb1*$^{Cre/+}$ or *Pax2-Cre*. Otic tissue is outlined in yellow; boxes indicate regions that are magnified in adjacent images. (**E**,**F**) NEC derivatives (green) express Ap2α (red). (E) Transverse sections through the trunk neural tube (NT) and dorsal root ganglion (DRG). Images on the right are higher magnification demonstrating expression of GFP with Ap2α in the DRG. (F) Lateral whole-mount views (left column) of the first and second branchial arches (BA1, BA2). Sagittal sections through the branchial arches (middle column) with magnified views of the BA2 mesoderm (right column). Nuclei are stained with DAPI (blue). ss, somite stage.

2004). *Pax2* is one of the earliest markers of the presumptive otic and epibranchial placode domains (Ohyama and Groves, 2004; Ohyama et al., 2007) and *Pax2-Cre* expression leads to extensive labeling of otic cells (Fig. 1D). *Wnt1-Cre*-, *Pax3*$^{Cre/+}$- and *Hoxb1*$^{Cre/+}$-labeled lineages contribute to known NCC derivatives such as the dorsal root ganglion (DRG, Fig. 1E) and branchial arch mesoderm (Fig. 1F), as determined by expression of the retinoic acid responsive transcription factor Ap2α (Fig. 1E,F). Derivatives of reporter cells labeled by *Hoxb1*$^{Cre/+}$ in the anterior region of the embryo are limited to the second branchial arch, consistent with their migration from rhombomere 4 (O'Gorman, 2005).

The *Wnt1-Cre* labeled population comprises too few cells to visualize in the inner ear by whole mount (Fig. 1A). Cells labeled by *Pax3*$^{Cre/+}$ can be seen but it is not clear whether GFP is in the OV or surrounding cells (Fig. 1B). Upon sectioning of embryos, NEC lineages in *Wnt1-Cre*, *Pax3*$^{Cre/+}$ and *Hoxb1*$^{Cre/+}$ mice were observed in the otic epithelium (Fig. 2A). Specifically, GFP reporter cells were localized to the prosensory epithelium of the OV as well as within the CVG. Fate mapping of the otic placode ectoderm by *Pax2-Cre* showed that the vast majority of cells in the otic placode appear to express GFP at E8.5; however, otic cells that were negative for GFP became evident at later otic cup and OV stages (Fig. 2A). *Wnt1-Cre* and *Pax3*$^{Cre/+}$ fate maps were confirmed with a *lacZ* reporter line, *Rosa26R* (Soriano, 1999), which shows a comparable distribution of reporter cells in the neurosensory region of the OV epithelium adjacent to the site of CVG formation, as well as within the CVG at E10.5 (Fig. 2B). Based on rough quantification of the total number of cells within the OV and CVG at E10.5 in *Pax3*$^{Cre/+}$;*RCE*$^{GFP/+}$ embryos, we estimate that NEC derivatives constitute ~20% of the total number of cells in the OV and ~25% of the total number of cells in the CVG (data not shown, illustrated in Fig. 2C).

We noted that *Pax3*$^{Cre/+}$ labels a more extensive population of NECs than *Wnt1-Cre* in the neural tube, OV and CVG (Figs 1A,B, 2A,B). This discrepancy is not obvious in other NCC derivatives such as the DRG and branchial arches (Fig. 1E,F). These results suggest that while both *Pax3*$^{Cre/+}$ and *Wnt1-Cre* can be used to fate map derivatives of NCCs that have been specified in the most dorsal part of the neural tube, *Pax3*$^{Cre/+}$ is additionally active in more ventral neural tube cells that may not necessarily have undergone NCC differentiation. This introduces the possibility that NECs, besides NCCs, may directly enter the otic epithelium from the neural tube.

It was important to rule out ectopic or leaky activity of Cre in otic tissue where *Wnt1* and *Pax3* are not normally expressed (Kwang et al., 2002; Tajbakhsh et al., 1998). Expression of *Cre* mRNA was assessed in *Wnt1-Cre* and *Pax3*$^{Cre/+}$ mice by in situ hybridization (Fig. 3A). *Cre* is strongly expressed in the neural tube

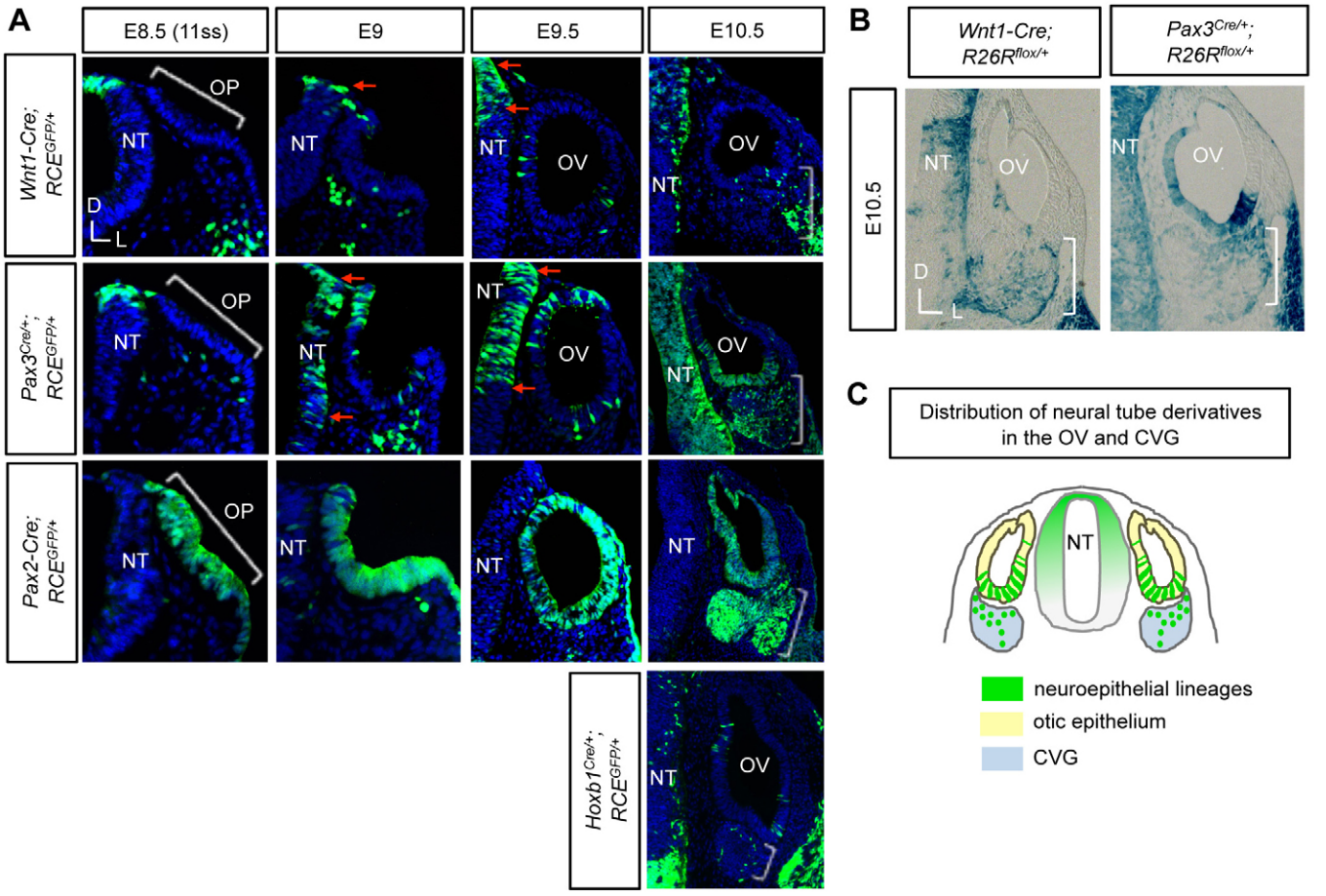

Fig. 2. NEC/NCC derivatives in the OV and CVG. (**A**) Transverse sections of embryos with GFP reporter expression (green). Brackets indicate the otic placode (OP) at E8.5 or the CVG at E10.5. Red arrows at E9 and E9.5 indicate the broader labeling of neural tube cells by *Pax3*$^{Cre/+}$ compared with *Wnt1-Cre*. Nuclei are stained with DAPI (blue). (**B**) *Wnt1-Cre* and *Pax3*$^{Cre/+}$ activation of the *R26R* is shown by X-gal staining. The CVG is indicated by brackets. (**C**) Illustration showing the distribution of NEC lineage derivatives (green) in the otic epithelium (yellow) and CVG (blue). NT, neural tube; ss, somite stage.

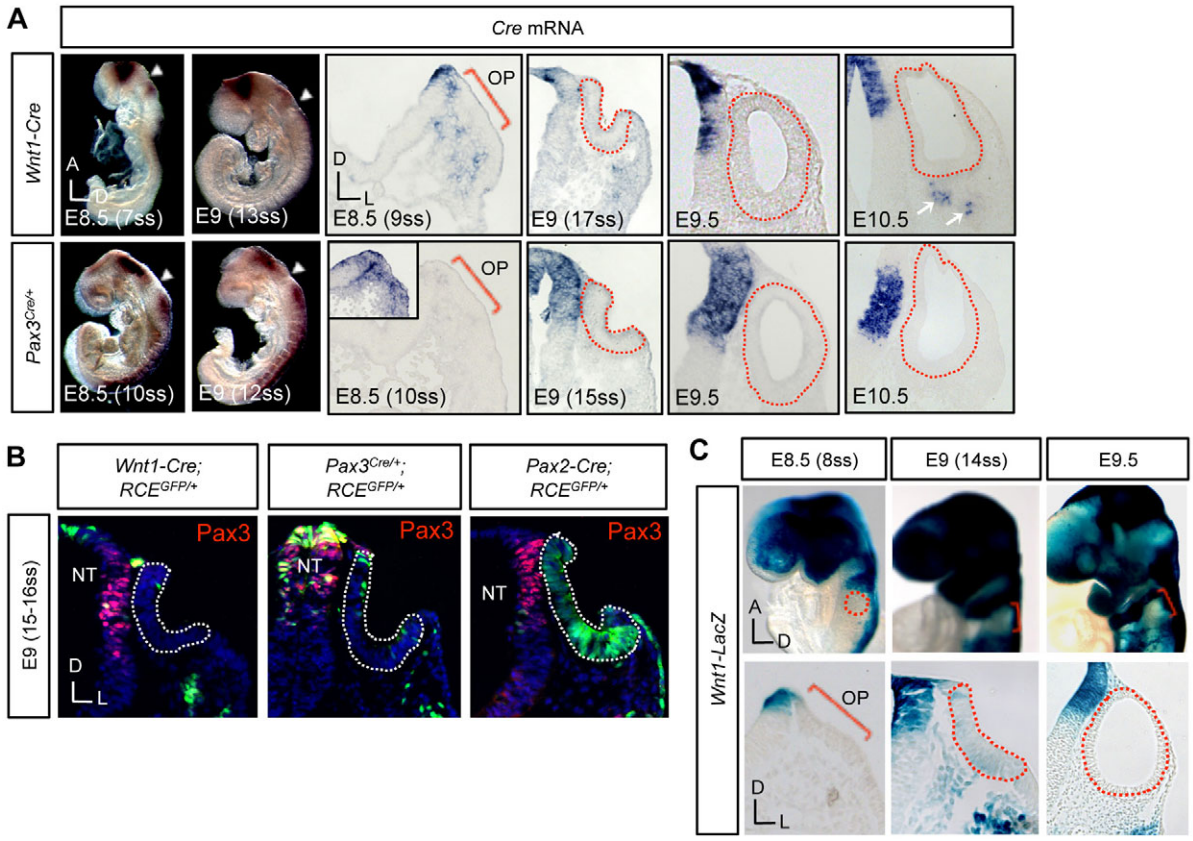

Fig. 3. *Wnt1-Cre* and *Pax3*$^{Cre/+}$ are not expressed in the otic epithelium. (**A**) Expression of *Cre* mRNA. Otic tissue is indicated on whole mounts (white arrowhead) and sections (red bracket, red outlines). In *Pax3*$^{Cre/+}$ mice at E8.5, the inset demonstrates strong expression in a more anterior section of the same embryo. *Wnt1-Cre* mice express *Cre* in the CVG at E10.5 (arrows). (**B**) Expression of endogenous Pax3 protein (red) in the neural tube (NT). The otic cup is outlined in white. Nuclei are stained with DAPI (blue). (**C**) Whole mounts and sections of *Wnt1-lacZ* embryos stained overnight for X-gal. Red brackets and dotted lines indicate otic tissue. ss, somite stage; OP, otic placode.

in both mouse lines and in the somites of *Pax3*$^{Cre/+}$. No *Cre* mRNA expression was detected in the otic epithelium from E8.5 to E10.5, thus implying that activation of the GFP reporter by Cre recombinase occurs within the neural tube prior to incorporation of NEC derivatives into the otic epithelium. We did see expression of *Cre* in the CVG of *Wnt1-Cre* mice at E10.5; however, this was not seen in *Pax3*$^{Cre/+}$ mice. Furthermore, we examined the normal expression of Pax3 protein at the otic cup stage in *Wnt1-Cre;RCE*$^{GFP/+}$, *Pax3*$^{Cre/+}$*;RCE*$^{GFP/+}$ and *Pax2-Cre;RCE*$^{GFP/+}$ mice (Fig. 3B). Pax3 was expressed in the neural tube, consistent with the expression of *Cre* mRNA, as driven by the endogenous *Pax3* regulatory elements (Fig. 3A). We did not observe expression of Pax3 in otic epithelial cells. Additionally, we performed X-gal staining of *Wnt1-lacZ* mice (Fig. 3C) in which a *lacZ* reporter recapitulates endogenous *Wnt1* expression (Echelard et al., 1994). Because it takes time for β-galactosidase to decay after *Wnt1-lacZ* is turned off, some NCC derivatives exhibit residual staining (Echelard et al., 1994). Even after overstaining, minimal X-gal staining was seen (note significantly darker staining in the neural tube where *Wnt1-lacZ* is still actively expressed, Fig. 3C).

Invasion of the otic epithelium by NECs during otic cup formation

Cranial NCCs migrate primarily from even-numbered rhombomeric segments of the hindbrain in both mouse and chick (Sechrist et al., 1993; Serbedzija et al., 1992). The OV is situated directly adjacent to rhombomere 5, which does not contribute significantly to migratory NCCs even though it is capable of generating them (Trainor et al., 2002). Fate mapping of *Hoxb1*$^{Cre/+}$ derivatives from rhombomere 4 to the OV and CVG was very similar to that of *Wnt1-Cre* derivatives at E10.5 (Fig. 2A). However, when we examined the anterior-posterior (AP) orientation of neural tube derivatives in the OV at E9.5 (Fig. 4A), we found that *Wnt1-Cre*-labeled NCCs and *Pax3*$^{Cre/+}$-labeled NECs were localized anteriorly, whereas *Hoxb1*$^{Cre/+}$ derivatives were located posteriorly.

In an attempt to capture the incorporation of neural tube cells into the otic epithelium in vivo, we used multiphoton microscopy for time-lapse imaging of live embryos (Wyckoff et al., 2007). *Pax3*$^{Cre/+}$*;RCE*$^{GFP/+}$ embryos were counterstained with red-fluorescent wheat germ agglutinin (WGA), a lectin that binds to sugar residues and is used to stain the plasma membrane of live cells. This allowed us to visualize the borders between neural tube epithelia, otic epithelia and mesenchyme. Time-lapse photography was performed for up to 3 hours with 5 μm optical sectioning (supplementary material Movies 1-4; Fig. 4B). Direct invasion of the developing otic cup by reporter cells from the neural tube was documented between the 12- to 14-somite stage (supplementary material Movies 1, 3-4; Fig. 4B). This time point coincides with the emigration of vital dye-labeled NCCs from the neural tube at the 11- to 14-somite stage in mice (Serbedzija et al., 1992), as well as at the stage when the otic epithelium is in direct contact with rhombomere 5 (Mayordomo et al., 1998) (Fig. 4B). Consistent with this is broken

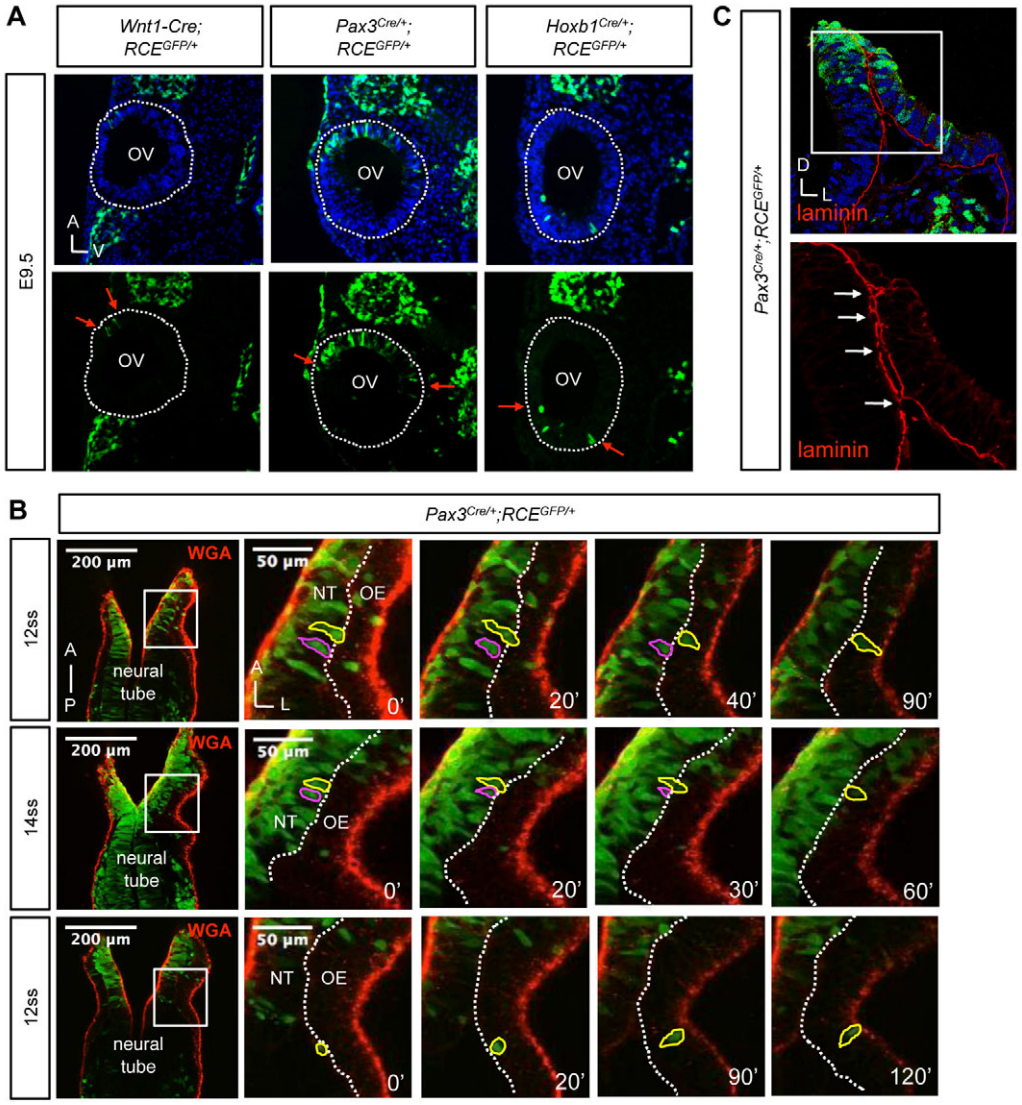

Fig. 4. AP orientation and invasion by NECs. (**A**) Sagittal sections of embryos. Red arrows indicate anterior versus posterior domains of reporter cell localization within the OV. Nuclei are stained with DAPI (blue). (**B**) *Pax3*$^{Cre/+}$;*RCE*$^{GFP/+}$ embryos were imaged with a multiphoton microscope. Three *z*-series (left to right) at different time-points. Original 25× fields are on the left (boxed areas are magnified). Boundaries between the neural tube (NT) and otic epithelium (OE) are indicated by broken white lines. Individual GFP$^+$ NECs from the level of rhombomere 5 (outlined in yellow) invade the otic epithelium whereas adjacent NECs (outlined in purple) emigrate into the mesenchyme. Corresponding time-lapse movies are included in the supplementary material (supplementary material Movies 1-4). (**C**) Confocal imaging of laminin protein (red) at E9 (15ss). The boxed region is shown at higher magnification. Arrows indicate breaks in laminin expression and fusion between the neuroepithelial and otic basal lamina. ss, somite stage.

expression of laminin where it appears that the basal lamina of the neuroepithelium is fused to that of the otic epithelium (Fig. 4C). There was also invasion of the otic epithelium by reporter cells in the mesenchyme, a process that would require mesenchymal-to-epithelial transition (supplementary material Movie 2). We cannot rule out the possibility that some neuroectodermal cells adjacent to the otic placode ectoderm are incorporated as the placode invaginates into the head during otic cup formation.

Localization of NEC/NCC derivatives in the developing mouse inner ear

Fate mapping through later stages of development (E11.5 to E17.5) revealed the distribution of *Wnt1-Cre* and *Pax3*$^{Cre/+}$ lineages during and after morphogenesis of the inner ear. *Wnt1-Cre* and *Pax3*$^{Cre/+}$ derivatives were localized to the CVG, the maculae of the saccule and utricle, and the cochlea (Fig. 5A,B). GFP reporter cells were also present in the ED at earlier stages (E11.5 to E14.5), but diminished by E17.5 (Fig. 5C). *Pax3*$^{Cre/+}$ derivatives were fate mapped around and within the cochlea, with many GFP reporter cells in the greater epithelial ridge (GER) as well as in the SV (Fig. 5C). We did not observe any *Wnt1-Cre* or *Pax3*$^{Cre/+}$-labeled derivatives in the SCCs or cristae at any stage.

We observed *Wnt1-Cre* and *Pax3*$^{Cre/+}$ GFP$^+$ derivatives in the periotic mesenchyme from E11.5 to E14.5 (Fig. 5A,B) in a manner that was similar to the known distribution of melanocytes around the inner ear (Steel et al., 1992; Stanchina et al., 2006). By E17.5, melanocytes are easily identified by their production of melanin. Pigmented reporter cells with distinctive dendritic-like morphology

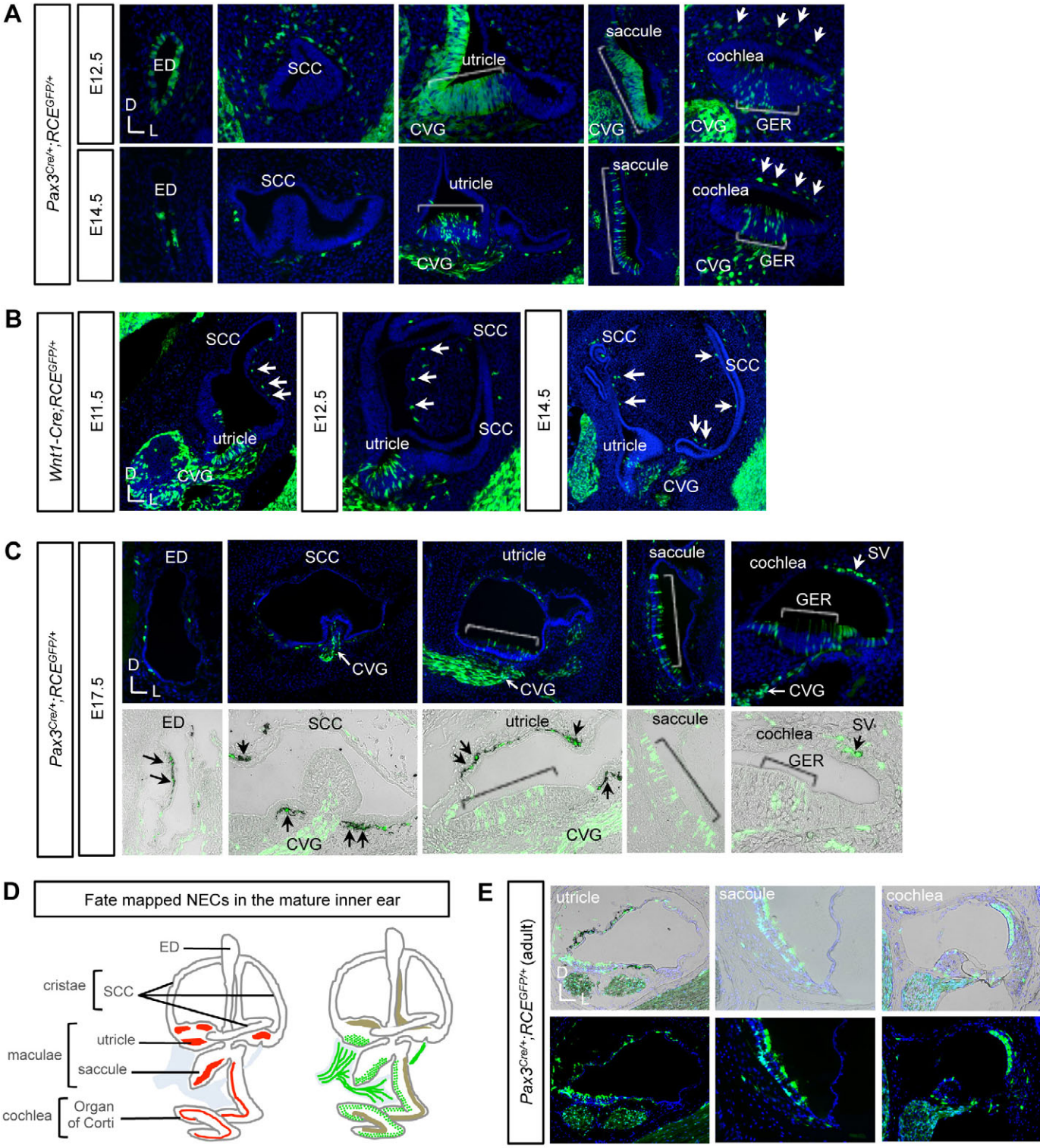

Fig. 5. NEC derivatives in the developing and mature inner ear. (**A**) Mapping of *Pax3*$^{Cre/+}$ derivatives (GFP, green). Sensory epithelia are indicated by brackets. Reporter cells are in the mesenchyme opposite the GER where the SV will form (arrows). (**B**) Mapping of *Wnt1-Cre* derivatives (GFP, green). Note GFP^{+} cells in the periotic mesenchyme (arrows) surrounding the developing SCCs. (**C**) NEC derivatives (GFP, green) in *Pax3*$^{Cre/+}$;*RCE*$^{GFP/+}$ mice remain in sensory epithelia (brackets). Bright-field (bottom) reveals pigment-producing melanocytes in the mesenchyme (arrows) surrounding the non-sensory epithelium and in the SV. (**D**) Illustration of the distribution of NEC derivatives (green) and NCC-derived melanocytes (brown) in the mature inner ear relative to sensory epithelia (red) and the CVG (blue). (**E**) Persistence of NEC derivatives (green) in the CVG, maculae and cochlea of adult mice (GFP overlaid with bright field). Nuclei are stained with DAPI (blue).

were identified in the mesenchyme surrounding the non-sensory epithelia of vestibular organs, as well as in the SV, but nowhere else within the inner ear epithelium or CVG (Fig. 5C). Melanocytes also express the GFP reporter as *Pax3*$^{Cre/+}$ labels NCCs all along the cranial and trunk neural tube (Fig. 1B,E,F). These results indicate that the NECs, and NCCs therein, that we are tracing in the inner ear sensory epithelium and CVG are not melanocytes (illustrated in Fig. 5D). We also fate mapped *Pax3*$^{Cre/+}$ labeled cells in the adult inner ear. Between 3 and 4 months of age (P96), *Pax3*$^{Cre/+}$ derivatives persisted in the utricular and saccular maculae, as well as in the CVG and organ of Corti (Fig. 5E).

Differentiation of NEC derivatives into specialized neurosensory cell types

The localization pattern of NEC derivatives in the developing inner ear suggested that they might function in neurosensory development. As specification of neuroblasts is one of the earliest cell fate determination events in the otic epithelium (Fekete and Wu, 2002), we first analyzed the expression of neural markers. Neurogenic differentiation factor 1 (NeuroD; Neurod1 – Mouse Genome Informatics) is a basic helix-loop-helix (bHLH) transcription factor expressed in neuroblasts both before and after delamination from the otic epithelium (Ma et al., 1998). Islet 1 (Isl1) is a LIM/homeodomain transcription factor expressed in CVG neuroblasts only after they have delaminated. A subset of the *Pax3*$^{Cre/+}$ and *Wnt1-Cre* lineage cells express NeuroD in the OV epithelium and CVG (Fig. 6A) suggesting that at least some GFP-expressing neuroblasts are specified from within the otic epithelium. Based on expression analysis of Isl1, we approximate that 80% of neuroblasts in the CVG derive from the otic placode ectoderm, as fate mapped by *Pax2-Cre*, whereas 20% derive from NECs, as fate mapped by *Pax3*$^{Cre/+}$ (Fig. 6B). *Pax3*$^{Cre/+}$- and *Wnt1-Cre*-labeled reporter cells appear to colocalize with neurofilament (NF), an intermediate filament that is strongly expressed in the axons of differentiating neurons (Fig. 6C). P75 is a neurotrophin receptor that is often used as a NCC marker and is also expressed in CVG neurons (Whitlon et al., 2010; Whitlon et al., 2009). P75 appears to colocalize with reporter cells in the CVG of *Wnt1-Cre;RCE*$^{GFP/+}$ mice (Fig. 6D), although some of this lineage may migrate from the mesoderm.

Next, we examined the expression of markers for other specialized neurosensory cell types. Myosin VIIA (MyoVIIA; Myo7a – Mouse Genome Informatics) is an unconventional myosin that is strongly expressed in all hair cells within the inner ear (Bermingham et al., 1999). Colocalization of MyoVIIA with GFP in *Pax3*$^{Cre/+}$-labeled reporter cells can be seen by confocal microscopy of whole-mount preparations (Fig. 7A) as well as tissue sections (Fig. 7B). The organ of Corti includes a single row of inner hair cells (IHC) and three rows of outer hair cells (OHCs) that run the length of the cochlea. Based on whole-mount immunofluorescence for MyoVIIA (Fig. 7A), it appears that NEC derivatives preferentially differentiate into IHCs versus OHCs. However, the general pattern of NEC derivatives differentiating into hair cells seems to be random within the organ of Corti and the maculae. Supporting cells that express P75 and the Ca^{2+}-binding protein S100 (White et al., 2006) and were found to be colocalized with *Pax3*$^{Cre/+}$-labeled reporter cells (Fig. 7C). Similar

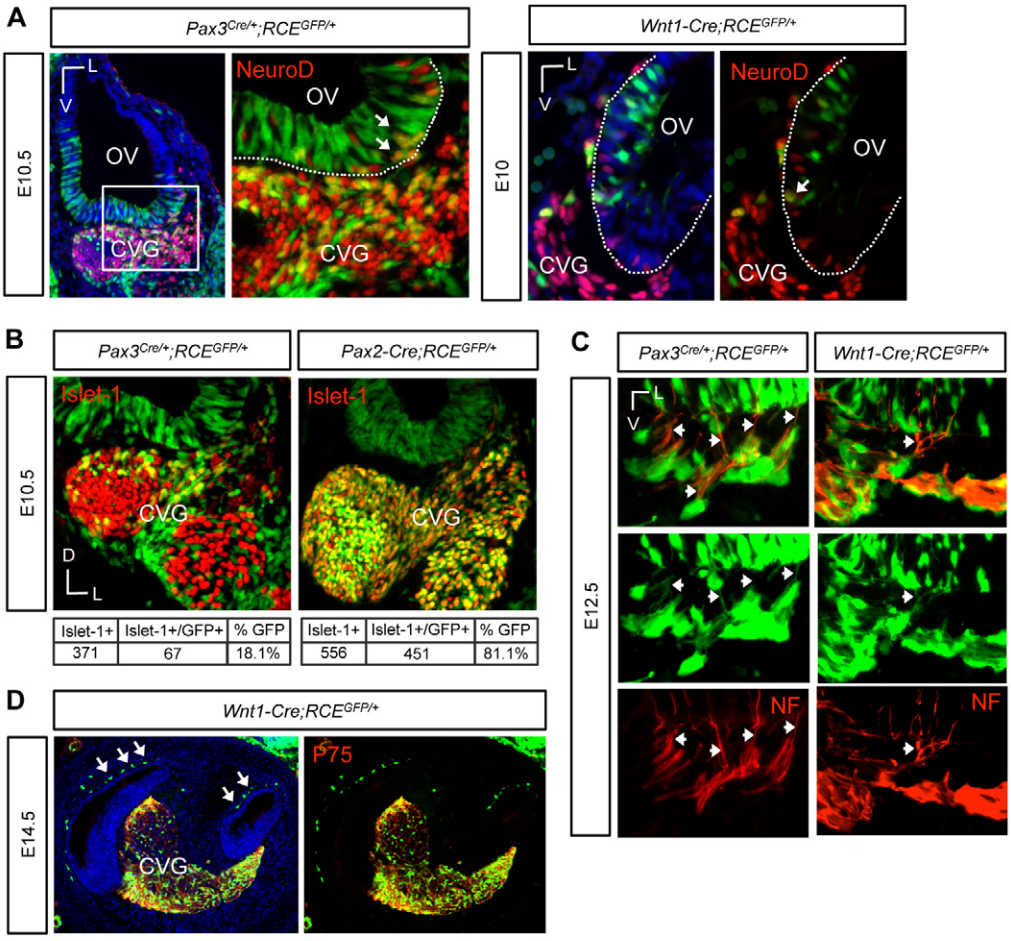

Fig. 6. NECs contribute neurons to the CVG. (**A**) Expression of NeuroD (red) in the otic epithelium (arrows) and CVG. Nuclei are stained with DAPI (blue). The boxed regions are shown on the right. Otic epithelium is outlined in white. (**B**) Expression of Islet-1. In the raw data images, ~18% of Islet-1-expressing neuroblasts in the CVG derive from NECs (left), whereas 80% derive from otic placode ectoderm (right). (**C**) Neurofilament (NF, red) and GFP (green) expression in CVG axons (arrows) protruding towards the utricle. (**D**) P75 (red) expression together with GFP (green) in the CVG. The image on the right is without DAPI. Mesenchymal GFP^{+} cells gather where the SV will form (arrows).

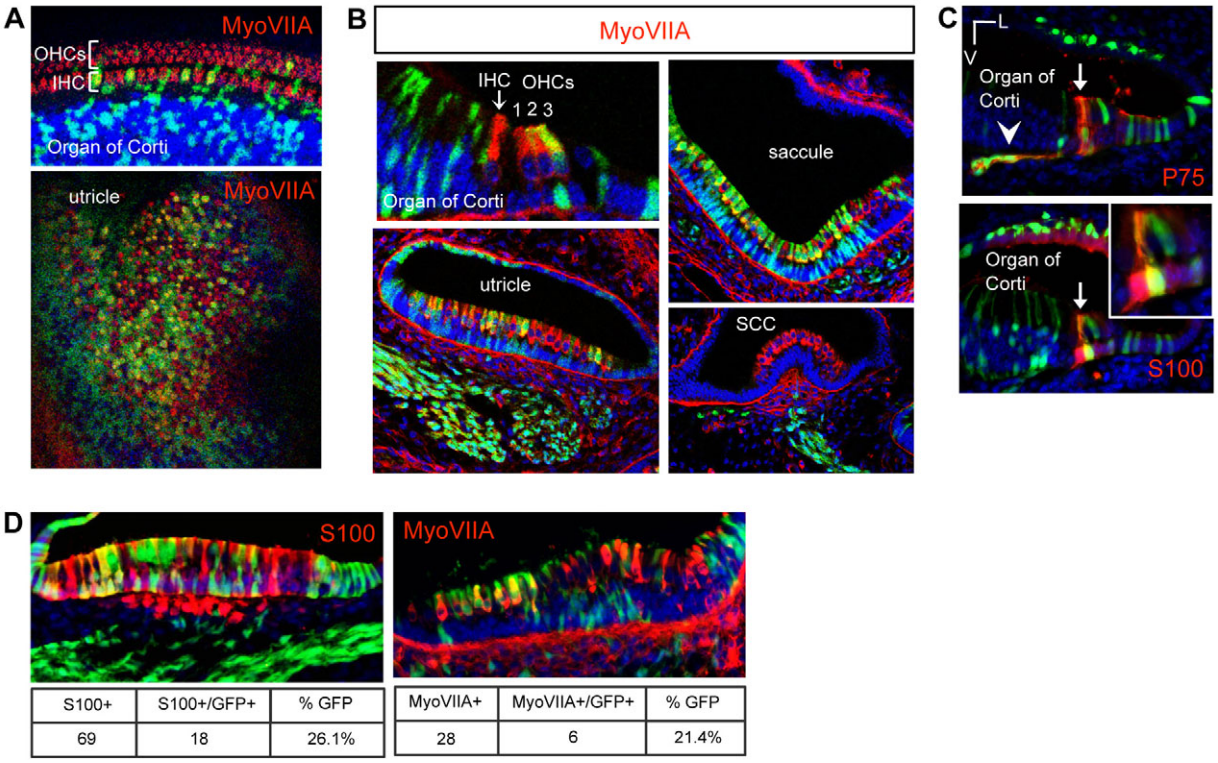

S100+	S100+/GFP+	% GFP
69	18	26.1%

MyoVIIA+	MyoVIIA+/GFP+	% GFP
28	6	21.4%

Fig. 7. Differentiation of NEC descendants into mechanosensory and supporting cells. (A-D) Immunofluorescence on *Pax3*$^{Cre/+}$;*RCE*$^{GFP/+}$ embryos at E17.5. Nuclei are stained with DAPI (blue). (**A**) Whole-mount immunofluorescence for MyoVIIA (red) on sensory epithelia from the utricle and cochlea. Images were taken using a confocal microscope. IHC, inner hair cell; OHCs, outer hair cells. (**B**) Confocal images of tissue sections. In the organ of Corti, numbers 1-3 indicate the OHCs and an arrow indicates the IHC. (**C**) Supporting cells (arrows) express P75 (red) and S100 (red). Arrowhead indicates NEC-derived neurons that express P75 projecting from the CVG. (**D**) Expression of S100 (red) and MyoVIIA (red) in utricles of *Pax3*$^{Cre/+}$;*RCE*$^{GFP/+}$ embryos at E17.5. In the raw data images, *Pax3*$^{Cre/+}$-labeled derivatives give rise to 26% of supporting cells and 21% of hair cells in the maculae.

to what was observed for hair cells, it appears that the distribution of supporting cells derived from the *Pax3*$^{Cre/+}$ lineage is randomized within the maculae and organ of Corti. We estimate that *Pax3*$^{Cre/+}$ derivatives account for ~25% of supporting cells and 20% of hair cells within the macula (Fig. 7D).

It is currently thought that glial cells within the CVG are NCC derived (Britsch et al., 2001; Breuskin et al., 2010; D'Amico-Martel and Noden, 1983). We sought to confirm this using our fate-mapping approach. Sox10 is a high-mobility group-domain transcription factor that is expressed in NCCs and is necessary for the survival of CVG glia (Breuskin et al., 2010). However, *Sox10* is also expressed throughout the OV (Breuskin et al., 2010). When we analyzed the expression of Sox10 protein in CVG nuclei, it was clear that all Sox10^{+} cells had been labeled by *Pax3*$^{Cre/+}$, although not all *Pax3*$^{Cre/+}$ reporter cells expressed Sox10 (Fig. 8A). When comparing this with the otic placode ectoderm lineage labeled by *Pax2-Cre*, we did not observe any GFP reporter cells that were also Sox10^{+} in the cochlear component of the CVG, but there were some cells with colocalization of Sox10 and GFP in the vestibular component (Fig. 8B).

DISCUSSION

In this study, we demonstrate for the first time that the mammalian inner ear originates from otic placode ectoderm and NECs, as determined by genetic labeling of neural tube populations by *Wnt1-Cre*, *Pax3*$^{Cre/+}$ and *Hoxb1*$^{Cre/+}$. This changes the current dogma – that only the otic placode ectoderm gives rise to the inner ear labyrinth and neurons of the CVG. Our results show that NEC lineages, which probably include NCCs, can invade the otic epithelium where they subsequently localize to the CVG, maculae and cochlea of the inner ear. Together with otic epithelium that originates from non-neural sensory placode ectoderm, cells that derive from the neural tube differentiate into neurons, hair cells and supporting cells. This is in addition to the known contributions of NCC lineages to: (1) the SV that surrounds the cochlea; and (2) glial cells of the CVG.

Dual origin of the OV and CVG

In vertebrate development, cranial sensory placodes are embryonic precursors of complex sensory organs (for a review, see Schlosser, 2010). NCCs are another embryonic population of cells that most probably co-evolved with sensory placodes in response to increased predatory behavior in vertebrates (Gans and Northcutt, 1983). It has been shown that NCCs cooperate with neurogenic (epibranchial and trigeminal) placodes for normal ganglia formation in mouse and chick (Begbie and Graham, 2001; Gammill et al., 2007; Shiau et al., 2008). In addition, neuromast formation in fish also requires cooperation between cells derived from the lateral line placode (present in fish only) and NCCs (Collazo et al., 1994; Grant et al., 2005).

Contribution of NCCs to other sensory organs is still being investigated. Only recently has it been shown by lineage tracing that glial ensheathing cells and subpopulations of neurons in the

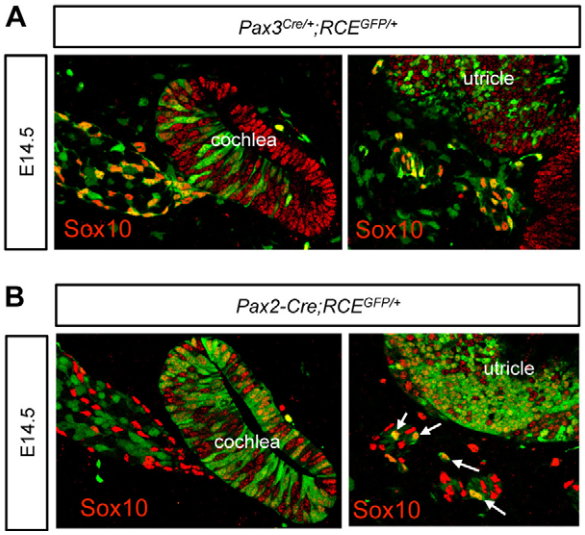

Fig. 8. Expression of Sox10 in the CVG. (**A**,**B**) Confocal images of Sox10 protein expression (red) in the CVG and otic epithelium at E14.5 in (A) *Pax3*$^{Cre/+}$;*RCE*$^{GFP/+}$ embryos and (B) *Pax2-Cre;RCE*$^{GFP/+}$ embryos. Arrows indicate otic placode ectoderm-derived cells that express Sox10 in the CVG.

olfactory system originate from NCCs that were fate mapped using *Wnt1-Cre* (Barraud et al., 2010; Forni et al., 2011). We also observed *Wnt1-Cre* and *Pax3*$^{Cre/+}$ derivatives in the olfactory epithelium in the course of our studies (supplementary material Fig. S1). In the lateral line, it is speculated that NCCs give rise to glia associated with sensory neuromasts; however, a direct lineage has not been shown.

Mixed origins of the CVG have been demonstrated by quail-chick grafting experiments (D'Amico-Martel and Noden, 1983). Presumptive placode ectoderm or neural crest was grafted from quail into chick to determine the cellular origin of sensory ganglia. It was noted that many of these experiments demonstrated chimeric formation of the CVG; however, this was attributed to incomplete transplant of the otic placode as there was also a mixture of donor and host cells in other parts of the inner ear. In light of our findings, these early grafting results in chick may have represented a true mixture of placode and NECs in the OV.

It has been debated whether or not a population of ventrally emigrating neural tube (VENT) cells exists that do not express the typical NCC marker HNK-1 (Dickinson et al., 2004). VENT cells have been proposed to migrate after NCCs and contribute to the OV and CVG, as well as to the cardiovascular system and enteric nervous system (Sohal et al., 2002; Ali et al., 2003a; Ali et al., 2003b; Sohal et al., 2002). Evidence for the existence of VENT cells has been challenged by some who question the accuracy of tracing techniques used to identify these cells in chick (Yaneza et al., 2002; Boot et al., 2003). The findings have not been further pursued until now.

Perhaps the most compelling evidence in the literature in support of our results is a study that was performed in zebrafish to dissect the functions of Sox10 in the inner ear (Dutton et al., 2009). Individual NCCs were labeled with rhodamine-dextran and a small percentage were traced to the otic epithelium. One cell was later found in a macula and another in the statoacoustic ganglion. These cells were deemed transient with no additional discussion. It is possible that only a small percentage of the NCCs were labeled, explaining a lower frequency than we have found using the Cre/loxP system in mice. When taken together, the data suggest that dual origin of the inner ear may extend beyond mammals to all vertebrates.

Fate-mapping techniques provide extensive information about cell lineages that cannot always be determined by gene expression analysis. Identification of NCCs by marker analysis is complicated by the changing expression profiles of migratory cells and by NCC-independent expression patterns during development. We were unable to identify NCCs in the OV based solely on expression analysis (supplementary material Fig. S2). Antibodies to Ap2α and the zinc-finger protein Snai1 exhibited staining in migratory NCC derivatives in the head mesenchyme but were not expressed by *Pax3*$^{Cre/+}$-labeled derivatives in the otic cup (supplementary material Fig. S2A,B). Similarly, mRNA expression of cellular retinoic acid-binding protein 1 (*Crabp1*) was not detected in the otic cup by in situ hybridization (supplementary material Fig. S2C). The AP orientation of NECs in the OV at E9.5 suggests a multifaceted contribution of NECs to the OV and CVG that: (1) probably includes cellular contributions from more than one rhombomere; and (2) may or may not include cells that have been specified as NCCs.

One way to demonstrate the presence of a second cell type in the OV is to use a Pax2-specific antibody. The *Pax2-Cre* transgene is expressed early in the otic placode ectoderm, whereas endogenous Pax2 protein is expressed in the otic placode and otic cup (Ohyama and Groves, 2004). At slightly later stages of OV development, endogenous Pax2 is localized ventrally where it is required for cochlear outgrowth (Burton et al., 2004). Unfortunately, Pax2 protein shows a dynamic expression pattern in the OV and, because of this, expression of Pax2 protein only partially overlaps with the *Pax2-Cre* fate map (supplementary material Fig. S2D). Vital dye-tracing experiments in chick have demonstrated significant mixing of cells fated to different tissues prior to specification and formation of the otic placode (Streit, 2002). Our results suggest that recruitment of cells from the neural tube occurs after otic placode formation. It is unclear whether or not NEC derivatives are also subject to otic specification signals.

Neurosensory development of the inner ear

Neurons and hair cells of the maculae derive from a common pool of neurosensory progenitors that express neurogenin 1 (*Ngn1*) (Raft et al., 2007). *Ngn1-Cre* derivatives are also localized to the CVG, maculae and GER of the cochlea, and are capable of giving rise to neurons, hair cells and supporting cells within the maculae (Raft et al., 2007). Results from our study show that localization and differentiation of NEC derivatives in the inner ear and CVG coincide with the known distribution of *Ngn1-Cre* fate-mapped cells (Raft et al., 2007). The cristae are sensory epithelia that are defined by expression of the morphogen *Bmp4*, which is essential for SCC formation (Matei et al., 2005; Chang et al., 2008). Neither the NEC lineages (this study) nor the *Ngn1-Cre* lineage (Raft et al., 2007) were found in the cristae or SCCs, indicating that this domain may be subject to regulatory mechanisms that are independent of those in the maculae or organ of Corti.

In the mature inner ear, NEC derivatives differentiate into neurons, hair cells and supporting cells; however, there was no single neurosensory cell type that derived exclusively from the neural tube lineages. Therefore, cellular fate within the neurosensory region of the inner ear appears to be independent of cellular origin. This indicates that NEC derivatives in the inner ear

may not function in cell fate specification, but instead may play a role in spatial organization of proneurosensory regions early during development. Alternatively, the contribution of neural tube cells to the proneurosensory region of the otic epithelium may be important for establishing proper communication and connectivity between the inner ear and hindbrain.

Possible functional requirements for neuroepithelial cells in the inner ear

The best way to test the functional requirements of NCCs in inner ear development would be to inhibit the contribution of NECs to the OV. *Pax3*$^{Cre/Cre}$ mice are functionally null but do not have defects in NCC migration (Serbedzija and McMahon, 1997). Nonetheless, *Splotch* (*Sp*^{2H}/*Sp*^{2H}) mice that are homozygous null for *Pax3* have been reported to have inner ear morphological defects and neuronal degeneration with phenotypic variability that corresponded with the severity of neural tube defects (Deol, 1966; Buckiova and Syka, 2004). We confirmed these findings by paintfilling of the inner ear labyrinth in *Pax3*$^{Cre/Cre}$-null mice (supplementary material Fig. S3). The hindbrain is essential for patterning the OV cell non-autonomously via secretion of morphogens such as Sonic hedgehog and Wnt (Vazquez-Echeverria et al., 2008; Riccomagno et al., 2002; Riccomagno et al., 2005; Liang et al., 2010). Therefore, analysis and phenotypic interpretation of *Pax3*-null mutants is complicated by the inability to isolate the requirements for direct NEC contribution versus cell non-autonomous signaling to the OV.

We did not attempt to ablate NCCs by *Wnt1* loss-of-function because *Wnt1*-null mice do not have defects in neural crest-derived tissues, probably owing to compensation by other Wnt genes in the neuroectoderm (McMahon and Bradley, 1990). Direct requirements of NCCs in inner ear development could not be tested within the scope of this study and will require alternative approaches, such as conditional cell ablation, to bypass defects in signaling from the hindbrain.

Origin of CVG glia

Glia of the CVG are known to be of NCC origin based on early chick-quail chimera studies (Britsch et al., 2001; Breuskin et al., 2010; D'Amico-Martel and Noden, 1983). Degeneration of glial cells in the CVG occurs in the absence of Sox10 (Breuskin et al., 2010). However, fate-mapping techniques have not been used in mice order to confirm the embryonic origin of these glia. Our results confirm that Sox10-expressing cells in the CVG are NCC derived, but that some cells from the otic placode ectoderm lineage also express Sox10 in the CVG. Our findings emphasize the need for further investigation of glial cell specification and development with respect to the inner ear.

Acknowledgements

We greatly thank Dr Gordon Fishell for the *RCE:LoxP* mouse line. We appreciate the intellectual discussions and training by Dr Jeffrey E. Segall and Jeffrey Wyckoff of the Intravital Imaging Core. We are indebted to helpful discussions with Raquel Castellanos, Dennis Monks and Stephania Macchiarulo. We thank Dr Sonja Nowotschin for critical reading of the manuscript.

Funding

This work was supported by the National Institutes of Health, National Institute on Deafness and other Communication Disorders [NIDCD R01 DC05186 to B.E.M.]. Antibodies obtained from the Developmental Studies Hybridoma Bank were developed under the auspices of the NICHD and maintained by The University of Iowa. This work was supported by the National Institutes of Health [NIDCD R01 DC05186 to B.E.M.]. Deposited in PMC for release after 12 months.

Competing interests statement

The authors declare no competing financial interests.

Supplementary material

Supplementary material available online at
http://dev.biologists.org/lookup/suppl/doi:10.1242/dev.069849/-/DC1

References

Ali, M. M., Jayabalan, S., Machnicki, M. and Sohal, G. S. (2003a). Ventrally emigrating neural tube cells migrate into the developing vestibulocochlear nerve and otic vesicle. *Int. J. Dev. Neurosci.* **21**, 199-208.

Ali, M. M., Farooqui, F. A. and Sohal, G. S. (2003b). Ventrally emigrating neural tube cells contribute to the normal development of heart and great vessels. *Vascul. Pharmacol.* **40**, 133-140.

Anniko, M. and Wikstrom, S. O. (1984). Pattern formation of the otic placode and morphogenesis of the otocyst. *Am. J. Otolaryngol.* **6**, 373-381.

Barald, K. F. and Kelley, M. W. (2004). From placode to polarization: new tunes in inner ear development. *Development* **131**, 4119-4130.

Barraud, P., Seferiadis, A. A., Tyson, L. D., Zwart, M. F., Szabo-Rogers, H. L., Ruhrberg, C., Liu, K. J. and Baker, C. V. (2010). Neural crest origin of olfactory ensheathing glia. *Proc. Natl. Acad. Sci. USA* **107**, 21040-21045.

Begbie, J. and Graham, A. (2001). Integration between the epibranchial placodes and the hindbrain. *Science* **294**, 595-598.

Bermingham, N. A., Hassan, B. A., Price, S. D., Vollrath, M. A., Ben-Arie, N., Eatock, R. A., Bellen, H. J., Lysakowski, A. and Zoghbi, H. Y. (1999). Math1: an essential gene for the generation of inner ear hair cells. *Science* **284**, 1837-1841.

Birgbauer, E., Sechrist, J., Bronner-Fraser, M. and Fraser, S. (1995). Rhombomeric origin and rostrocaudal reassortment of neural crest cells revealed by intravital microscopy. *Development* **121**, 935-945.

Boot, M. J., Gittenberger-de Groot, A. C., van Iperen, L. and Poelmann, R. E. (2003). The myth of ventrally emigrating neural tube (VENT) cells and their contribution to the developing cardiovascular system. *Anat. Embryol. (Berl.)* **206**, 327-333.

Breuskin, I., Bodson, M., Thelen, N., Thiry, M., Borgs, L., Nguyen, L., Stolt, C., Wegner, M., Lefebvre, P. P. and Malgrange, B. (2010). Glial but not neuronal development in the cochleo-vestibular ganglion requires Sox10. *J. Neurochem.* **114**, 1827-1839.

Britsch, S., Goerich, D. E., Riethmacher, D., Peirano, R. I., Rossner, M., Nave, K. A., Birchmeier, C. and Wegner, M. (2001). The transcription factor Sox10 is a key regulator of peripheral glial development. *Genes Dev.* **15**, 66-78.

Bronner-Fraser, M. (1995). Origins and developmental potential of the neural crest. *Exp. Cell Res.* **218**, 405-417.

Buckiova, D. and Syka, J. (2004). Development of the inner ear in Splotch mutant mice. *Neuroreport* **15**, 2001-2005.

Burton, Q., Cole, L. K., Mulheisen, M., Chang, W. and Wu, D. K. (2004). The role of Pax2 in mouse inner ear development. *Dev. Biol.* **272**, 161-175.

Cable, J., Barkway, C. and Steel, K. P. (1992). Characteristics of stria vascularis melanocytes of viable dominant spotting (Wv/Wv) mouse mutants. *Hear. Res.* **64**, 6-20.

Cable, J., Jackson, I. J. and Steel, K. P. (1995). Mutations at the W locus affect survival of neural crest-derived melanocytes in the mouse. *Mech. Dev.* **50**, 139-150.

Chang, W., Lin, Z., Kulessa, H., Hebert, J., Hogan, B. L. and Wu, D. K. (2008). Bmp4 is essential for the formation of the vestibular apparatus that detects angular head movements. *PLoS Genet.* **4**, e1000050.

Collazo, A., Fraser, S. E. and Mabee, P. M. (1994). A dual embryonic origin for vertebrate mechanoreceptors. *Science* **264**, 426-340.

D'Amico-Martel, A. and Noden, D. M. (1983). Contributions of placodal and neural crest cells to avian cranial peripheral ganglia. *Am. J. Anat.* **166**, 445-468.

Danielian, P. S., Muccino, D., Rowitch, D. H., Michael, S. K. and McMahon, A. P. (1998). Modification of gene activity in mouse embryos in utero by a tamoxifen-inducible form of Cre recombinase. *Curr. Biol.* **8**, 1323-1326.

Deol, M. S. (1966). Influence of the neural tube on the differentiation of the inner ear in the mammalian embryo. *Nature* **209**, 219-220.

Dickinson, D. P., Machnicki, M., Ali, M. M., Zhang, Z. and Sohal, G. S. (2004). Ventrally emigrating neural tube (VENT) cells: a second neural tube-derived cell population. *J. Anat.* **205**, 79-98.

Dutton, K., Abbas, L., Spencer, J., Brannon, C., Mowbray, C., Nikaido, M., Kelsh, R. N. and Whitfield, T. T. (2009). A zebrafish model for Waardenburg syndrome type IV reveals diverse roles for Sox10 in the otic vesicle. *Dis. Model. Mech.* **2**, 68-83.

Echelard, Y., Vassileva, G. and McMahon, A. P. (1994). Cis-acting regulatory sequences governing Wnt-1 expression in the developing mouse CNS. *Development* **120**, 2213-2224.

Engleka, K. A., Gitler, A. D., Zhang, M., Zhou, D. D., High, F. A. and Epstein, J. A. (2005). Insertion of Cre into the Pax3 locus creates a new allele of Splotch and identifies unexpected Pax3 derivatives. *Dev. Biol.* **280**, 396-406.

Fekete, D. M. and Wu, D. K. (2002). Revisiting cell fate specification in the inner ear. *Curr. Opin. Neurobiol.* **12**, 35-42.
Forni, P. E., Taylor-Burds, C., Melvin, V. S., Williams, T. and Wray, S. (2011). Neural crest and ectodermal cells intermix in the nasal placode to give rise to GnRH-1 neurons, sensory neurons, and olfactory ensheathing cells. *J. Neurosci.* **31**, 6915-6927.
Franco, D., de Boer, P. A., de Gier-de Vries, C., Lamers, W. H. and Moorman, A. F. (2001). Methods on in situ hybridization, immunohistochemistry and beta-galactosidase reporter gene detection. *Eur. J. Morphol.* **39**, 3-25.
Gammill, L. S., Gonzalez, C. and Bronner-Fraser, M. (2007). Neuropilin 2/semaphorin 3F signaling is essential for cranial neural crest migration and trigeminal ganglion condensation. *Dev. Neurobiol.* **67**, 47-56.
Gans, C. and Northcutt, R. G. (1983). Neural crest and the origin of vertebrates: a new head. *Science* **220**, 268-273.
Goulding, M. D., Chalepakis, G., Deutsch, U., Erselius, J. R. and Gruss, P. (1991). Pax-3, a novel murine DNA binding protein expressed during early neurogenesis. *EMBO J.* **10**, 1135-1147.
Graham, A., Begbie, J. and McGonnell, I. (2004). Significance of the cranial neural crest. *Dev. Dyn.* **229**, 5-13.
Grant, K. A., Raible, D. W. and Piotrowski, T. (2005). Regulation of latent sensory hair cell precursors by glia in the zebrafish lateral line. *Neuron* **45**, 69-80.
Kwang, S. J., Brugger, S. M., Lazik, A., Merrill, A. E., Wu, L. Y., Liu, Y. H., Ishii, M., Sangiorgi, F. O., Rauchman, M., Sucov, H. M. et al. (2002). Msx2 is an immediate downstream effector of Pax3 in the development of the murine cardiac neural crest. *Development* **129**, 527-538.
Le Douarin, N. M. (1986). Investigations on the neural crest. Methodological aspects and recent advances. *Ann. N. Y. Acad. Sci.* **486**, 66-86.
Liang, J. K., Bok, J. and Wu, D. K. (2010). Distinct contributions from the hindbrain and mesenchyme to inner ear morphogenesis. *Dev. Biol.* **337**, 324-334.
Ma, Q., Chen, Z., del Barco Barrantes, I., de la Pompa, J. L. and Anderson, D. J. (1998). neurogenin1 is essential for the determination of neuronal precursors for proximal cranial sensory ganglia. *Neuron* **20**, 469-482.
Matei, V., Pauley, S., Kaing, S., Rowitch, D., Beisel, K. W., Morris, K., Feng, F., Jones, K., Lee, J. and Fritzsch, B. (2005). Smaller inner ear sensory epithelia in Neurog 1 null mice are related to earlier hair cell cycle exit. *Dev. Dyn.* **234**, 633-650.
Mayordomo, R., Rodriguez-Gallardo, L. and Alvarez, I. S. (1998). Morphological and quantitative studies in the otic region of the neural tube in chick embryos suggest a neuroectodermal origin for the otic placode. *J. Anat.* **193**, 35-48.
McMahon, A. P. and Bradley, A. (1990). The Wnt-1 (int-1) proto-oncogene is required for development of a large region of the mouse brain. *Cell* **62**, 1073-1085.
Morsli, H., Choo, D., Ryan, A., Johnson, R. and Wu, D. K. (1998). Development of the mouse inner ear and origin of its sensory organs. *J. Neurosci.* **18**, 3327-3335.
O'Gorman, S. (2005). Second branchial arch lineages of the middle ear of wild-type and Hoxa2 mutant mice. *Dev. Dyn.* **234**, 124-131.
Ohyama, T. and Groves, A. K. (2004). Generation of Pax2-Cre mice by modification of a Pax2 bacterial artificial chromosome. *Genesis* **38**, 195-199.
Ohyama, T., Groves, A. K. and Martin, K. (2007). The first steps towards hearing: mechanisms of otic placode induction. *Int. J. Dev. Biol.* **51**, 463-472.
Raft, S., Koundakjian, E. J., Quinones, H., Jayasena, C. S., Goodrich, L. V., Johnson, J. E., Segil, N. and Groves, A. K. (2007). Cross-regulation of Ngn1 and Math1 coordinates the production of neurons and sensory hair cells during inner ear development. *Development* **134**, 4405-4415.
Riccomagno, M. M., Martinu, L., Mulheisen, M., Wu, D. K. and Epstein, D. J. (2002). Specification of the mammalian cochlea is dependent on Sonic hedgehog. *Genes Dev.* **16**, 2365-2378.
Riccomagno, M. M., Takada, S. and Epstein, D. J. (2005). Wnt-dependent regulation of inner ear morphogenesis is balanced by the opposing and supporting roles of Shh. *Genes Dev.* **19**, 1612-1623.
Sauka-Spengler, T. and Bronner-Fraser, M. (2008). A gene regulatory network orchestrates neural crest formation. *Nat. Rev. Mol. Cell Biol.* **9**, 557-568.
Schlosser, G. (2010). Making senses development of vertebrate cranial placodes. *Int. Rev. Cell Mol. Biol.* **283**, 129-234.
Schneider-Maunoury, S. and Pujades, C. (2007). Hindbrain signals in otic regionalization: walk on the wild side. *Int. J. Dev. Biol.* **51**, 495-506.
Sechrist, J., Serbedzija, G. N., Scherson, T., Fraser, S. E. and Bronner-Fraser, M. (1993). Segmental migration of the hindbrain neural crest does not arise from its segmental generation. *Development* **118**, 691-703.
Serbedzija, G. N. and McMahon, A. P. (1997). Analysis of neural crest cell migration in Splotch mice using a neural crest-specific LacZ reporter. *Dev. Biol.* **185**, 139-147.
Serbedzija, G. N., Bronner-Fraser, M. and Fraser, S. E. (1992). Vital dye analysis of cranial neural crest cell migration in the mouse embryo. *Development* **116**, 297-307.
Shiau, C. E., Lwigale, P. Y., Das, R. M., Wilson, S. A. and Bronner-Fraser, M. (2008). Robo2-Slit1 dependent cell-cell interactions mediate assembly of the trigeminal ganglion. *Nat. Neurosci.* **11**, 269-276.
Sohal, G. S., Ali, M. M. and Farooqui, F. A. (2002). A second source of precursor cells for the developing enteric nervous system and interstitial cells of Cajal. *Int. J. Dev. Neurosci.* **20**, 619-626.
Soriano, P. (1999). Generalized lacZ expression with the ROSA26 Cre reporter strain. *Nat. Genet.* **21**, 70-71.
Sousa, V. H., Miyoshi, G., Hjerling-Leffler, J., Karayannis, T. and Fishell, G. (2009). Characterization of Nkx6-2-derived neocortical interneuron lineages. *Cereb. Cortex* **19 Suppl. 1**, i1-i10.
Stanchina, L., Baral, V., Robert, F., Pingault, V., Lemort, N., Pachnis, V., Goossens, M. and Bondurand, N. (2006). Interactions between Sox10, Edn3 and Ednrb during enteric nervous system and melanocyte development. *Dev. Biol.* **295**, 232-249.
Steel, K. P. and Barkway, C. (1989). Another role for melanocytes: their importance for normal stria vascularis development in the mammalian inner ear. *Development* **107**, 453-463.
Streit, A. (2002). Extensive cell movements accompany formation of the otic placode. *Dev. Biol.* **249**, 237-254.
Tajbakhsh, S., Borello, U., Vivarelli, E., Kelly, R., Papkoff, J., Duprez, D., Buckingham, M. and Cossu, G. (1998). Differential activation of Myf5 and MyoD by different Wnts in explants of mouse paraxial mesoderm and the later activation of myogenesis in the absence of Myf5. *Development* **125**, 4155-4162.
Trainor, P. A., Sobieszczuk, D., Wilkinson, D. and Krumlauf, R. (2002). Signalling between the hindbrain and paraxial tissues dictates neural crest migration pathways. *Development* **129**, 433-442.
Vazquez-Echeverria, C., Dominguez-Frutos, E., Charnay, P., Schimmang, T. and Pujades, C. (2008). Analysis of mouse kreisler mutants reveals new roles of hindbrain-derived signals in the establishment of the otic neurogenic domain. *Dev. Biol.* **322**, 167-178.
White, P. M., Doetzlhofer, A., Lee, Y. S., Groves, A. K. and Segil, N. (2006). Mammalian cochlear supporting cells can divide and trans-differentiate into hair cells. *Nature* **441**, 984-987.
Whitlon, D. S., Tieu, D., Grover, M., Reilly, B. and Coulson, M. T. (2009). Spontaneous association of glial cells with regrowing neurites in mixed cultures of dissociated spiral ganglia. *Neuroscience* **161**, 227-235.
Whitlon, D. S., Tieu, D. and Grover, M. (2010). Purification and transfection of cochlear Schwann cells. *Neuroscience* **171**, 23-30.
Wikstrom, S. O. and Anniko, M. (1987). Early development of the stato-acoustic and facial ganglia. *Acta Otolaryngol.* **104**, 166-174.
Wilson, Y. M., Richards, K. L., Ford-Perriss, M. L., Panthier, J. J. and Murphy, M. (2004). Neural crest cell lineage segregation in the mouse neural tube. *Development* **131**, 6153-6162.
Wyckoff, J. B., Wang, Y., Lin, E. Y., Li, J. F., Goswami, S., Stanley, E. R., Segall, J. E., Pollard, J. W. and Condeelis, J. (2007). Direct visualization of macrophage-assisted tumor cell intravasation in mammary tumors. *Cancer Res.* **67**, 2649-2656.
Yaneza, M., Gilthorpe, J. D., Lumsden, A. and Tucker, A. S. (2002). No evidence for ventrally migrating neural tube cells from the mid- and hindbrain. *Dev. Dyn.* **223**, 163-167.

Table S1. Primers for genotyping

Genotype	Primer	Sequence (5′ to 3′)
Pax3$^{Cre/+}$	oIMR6977common	CTGCACTCAAGGGACTCCTC
	oIMR6978wtRev	GTGAAGGCGAGACGAAAAAG
	oIMR9074mutRev	AGGCAAATTTTGGTGTACGG
Wnt1-lacZ	Lacz-Fwd	ATCCTCTGCATGGTCAGGTC
	Lacz-Rev	CGTGGCCTGATTCATTCC
Hoxb1$^{Cre/+}$	EBCreFwd	CAATGCTGTTTCACTGGTTATG
	EBCreRev	CATTGCCCCTGTTTCACTATC
RCE:LoxP	RCE-Rosa1	CCCAAAGTCGCTCTGAGTTGTTATC
	RCE-Rosa2	GAAGGAGCGGGAGAAATGGATATG
	RCE-Cag3	CCAGGCGGGCCATTTACCGTAAG